Chinese Chemical Letters 32 (2021) 787–790

Contents lists available at ScienceDirect

Chinese Chemical Letters

journal homepage: www.elsevier.com/locate/cclet

Communication

Microwave-assisted acid-induced formation of linker vacancies within Zr-based metal organic frameworks with enhanced heterogeneous catalysis

Yu Liang[a], Chenhui Li[a], Lanjun Chen[a], Jia Huo[a,b,*], Mohammed Loubidi[a], Yangyang Zhou[a], Yanbo Liu[a]

[a] State Key Laboratory of Chem/Bio-sensing and Chemometrics, College of Chemistry and Chemical Engineering, Hunan University, Changsha 410082, China
[b] Hunan Provincial Key Laboratory of Advanced Materials for New Energy Storage and Conversion, Hunan University of Science and Technology, Xiangtan 411201, China

ARTICLE INFO

Article history:
Received 8 April 2020
Received in revised form 11 June 2020
Accepted 30 June 2020
Available online 1 July 2020

Keywords:
Metal-organic frameworks
Microwave
Acid etching
Linker vacancy
Stability
Heterogeneous catalysis

ABSTRACT

Herein, we report a microwave-assisted acid-induced post-treatment method for the formation of linker vacancies within Zr-based metal organic frameworks (Zr-MOFs). The number of linker vacancies can be easily regulated with this method by changing the concentration of the HCl solution and the duration of microwave irradiation. The optimized defective UiO-66 showed higher linker defects with a higher specific surface area and thermal stability. The results of the catalytic cyclization of citronella showed that the Zr-MOFs with more defects exhibited enhanced catalytic performance. This work may provide a new method for the creation of defective MOFs with high activity and stability.

Metal organic frameworks (MOFs) are a kind of crystal materials with porous structure formed by coordination of metal ions or clusters with organic linkers [1,2]. Owing to the merits of presence of rich unsaturated metal active sites, chemically modifiability, high specific surface areas, and ordered porosity, these materials have attracted intensive attention in the fields of heterogeneous catalysis [3–5], adsorption/separation [6,7], drug delivery [8], sensing [9], and so on. However, their widespread applications still suffers from the hydrostatic stability, because the formation of frameworks is resulted from the weak coordination interaction, which makes MOFs very sensitive to moisture [7,10]. Long-term efforts have finally led to the successful preparation of UiO-66 [11], a 12-coordinated zirconium-based MOF, which is highly stable when exposed to 400 °C under air and aqueous solutions (neutral, or even acidic and basic solutions), reminiscent of a kind of industrially used porous materials, zeolites. This principle could be applied to prepare a series of water-stable zirconium-based metal organic frameworks, which have been used as supports for immobilization of catalytically active sites, such as metal nanoparticles and molecular catalysts [12–14].

The intrinsic catalytic activity of MOFs often originates from the unsaturated metal active sites serving as Lewis acids for heterogeneous catalysis. However, the activity of metal components of Zr-MOFs is seriously weakened by the fully saturated eight-coordination-environment of each zirconium atom in the frameworks [11]. Defect engineering, referring to the application of controlled defects (such as vacancies, dopants and lattice disorders), has recently been applied to create unsaturated metal sites in the metal oxides and MOFs for improving electrocatalysis and heterogeneous catalysis, respectively. Missing linker in the structure is an effective strategy to create defects for improving the catalytic performance of MOFs. For instance, De Vos *et al.* [15] demonstrated that pristine UiO-66 almost displayed no activity for the Meerwein reduction of 4-*tert*-butylcyclohexane with isopropanol (only 5% conversion after 24 h), whereas, the conversion rate reached 70% for defective UiO-66. Van Speybroeck *et al.* [16,17] further confirmed the condensation reaction of benzaldehyde and heptyl crossol aldehyde was only carried out for UiO-66 with ligand vacancies and consequent unsaturated Lewis acid sites on Zr^{4+} by combination of experimental and theoretical studies. Typically, ligand vacancies can be created through the "*de novo*" synthesis and postsynthetic treatment [18]. De Vos *et al.* developed

* Corresponding author at: State Key Laboratory of Chem/Bio-sensing and Chemometrics, College of Chemistry and Chemical Engineering, Hunan University, Changsha, 410082, China.
E-mail address: jiahuo@hnu.edu.cn (J. Huo).

https://doi.org/10.1016/j.cclet.2020.06.042
1001-8417/

a modulation approach to create linker vacancies within UiO-66 in the presence of trifluoroacetic acid and HCl during the synthesis, which significantly promote the conversion of citronellal to 3-methyl-1,3-butanediol compared with UiO-66 synthesized without the modulator [15]. Feng *et al.* [19] employed a hemilabile linker (4-sulfonatobenzoate) to synthesize a hemilabile UiO-66, the defects of which could be created through a postsynthetic treatment with H_2SO_4. Liang *et al.* [20] promoted the formation of ultrafine metal oxide nanoparticles by thermal decomposition of the linker, ultrasmall metal oxide nanoparticles immobilized in an open framework that exhibits high catalytic activity for Lewis acid-catalyzed reactions. Nonetheless, the postsynthetic treatment is not achievable for directly producing defects within pristine UiO-66 by consideration of the robust stability even within acidic solutions. Now, we develop a microwave-assisted acid-induced post-treated method for formation of linker vacancies within Zr-based metal organic frameworks. The physical characterization proves that the MOF materials with abundant unsaturated metal active sites can be obtained by this post-treatment method. Therefore, these MOF materials have better catalytic performance.

The following is the synthesis method of UiO-66 and MOF-808. Firstly, the synthesis of UiO-66 is 207 mg $ZrOCl_2{\cdot}8H_2O$ was weighed and dissolved in 20 mL *N*,*N*-dimethylformamide (DMF), then 5 cm^3 acetic acid was added and ultrasonic treatment was conducted until the solution was completely dissolved. Then weigh 120 mg of terephthalic acid into the mixture and conduct ultrasound for 20 min until it is completely dissolved. The mixture was transferred into a bottle with bag cover of 30 cm^3 and reacted in the oven at 120 °C for 24 h. After it was naturally cooled to room temperature, the white sample was obtained by centrifugation. After being washed in DMF for three times, the mixture was soaked in acetone for three times, each time for 12 h. After vacuum drying at 60 °C for 12 h, white UiO-66 powder was obtained. Vacuum drying at 200 °C for 24 h removed the adsorbed high boiling solvent molecules from the sample.

Then, MOF-808 was synthesized according to existing reports. 1.042 g H_3BTC and 1.94 g $ZrOCl_2{\cdot}8H_2O$ were dissolved in the mixture of formic acid/DMF (45 cm^3/45 cm^3). After the mixture was completely dissolved and mixed evenly, the mixture was divided into two sealed reaction reactors of 100 cm^3 and reacted in the oven at 130 °C for 48 h. After cooling to room temperature, wash with DMF three times, soak in acetone, and replace acetone once for 12 h, a total of three times. After drying at 60 °C for 12 h, the white powder was dried again at 200 °C for 12 h.

Next, the process of microwave acid treatment of MOF was HCl solutions of different concentrations were prepared, which were 0.01, 0.1, 0.5, 1 mol/L, respectively. Weigh 100 mg of UiO-66 sample powder and pour it into the microwave tube. Then measure 20 mL 0.5 mol/L hydrochloric acid solution into the microwave tube and stir magnetically for 10 min until the UiO-66 powder is completely dispersed in the hydrochloric acid solution. Finally, the closed microwave tube was put into the reactor, and the reaction conditions were set as 100 W, 100 °C, and the reaction time was from 30 min to 3 h. After cooling, the solution was centrifuged, washed with ultra-pure water, and ultrasonic. The operation was repeated for several times until the solution became neutral. Vacuum drying at 60 °C for 12 h, and then again drying at 200 °C and 12 h for activation. Similarly, MOF-808 was treated with a similar method. hydrochloric acid solution of 0.1 mol/L was selected and microwaved for 30 min, 1 h and 2 h respectively to obtain samples with different treatment times. The microwave reactor used in this experiment is Discover SP (CEM, U. S. A.).

Finally, the catalytic performance of different materials were tested by cyclization of citronella aldehyde. A solution of toluene containing citronellal was added to a three-mouth flask containing 10 mL glass containing MOF. For each catalyst, the ratio of citronellal to Zr is 15:1. After the reaction mixture is introduced, the flask is connected with the reflux condensing device, placed in an oil bath at 110 °C and stirred. Every certain time, the reaction liquid of about 0.2 mL was taken and filtered through a 200 nm filter to obtain the samples to be tested and analyzed by gas chromatography (Shandong Lunan SP-7890, FID).

Motivated by the principle of microwave interaction, we expected that strong coordination bonds between Zr and O could be broken upon the strong oscillation of acidic polar molecules (such as HCl) generated with microwave. Herein, we demonstrated that the microwave irradiation could promote effectively the acid-induced formation of linker vacancies within UiO-66. The number of linker vacancies can be regulated through changing the irradiation time and the concentration of HCl solution. It is found that increasing the irradiation time and the concentration of HCl solution can increase the number of linker defects, and the optimal condition is 0.5 mol/L HCl solution for 1 h under microwave irradiation, where defective UiO-66 displays the largest specific surface area with desirable linker vacancies (number of linker vacancies is 5.0 *vs.* 1.8 for pristine UiO-66). The optimized defective UiO-66 contains more exposed unsaturated Zr^{4+} active sites, which can serve as an effective Lewis acid for cyclization of citronella to 3-methyl-1,3-butanediol (Fig. 1). This defective UiO-66 show significantly improved catalytic activity with a conversion of 68.1% compared with that of 5.4% for pristine UiO-66. Whatever, the microwave-assisted acid induction strategy represents an effective method to create rich linker vacancies to expose more Lewis acid active sites for heterogeneous catalysis.

We selected UiO-66 as an initial model to create defective Zr-based MOFs with linker vacancies. Defective UiO-66 was synthesized with a two-step procedure. UiO-66 was first prepared with a typical solvothermal reaction (hereafter abbreviated as UiO-66_{ST}), which was subsequently treated with an HCl aqueous solution under the microwave irradiation at 100 °C to produce defective UiO-66 (noted as UiO-$66_{MW\text{-}mMnh}$, where M and h represent the concentration of the HCl aqueous solution and the irradiation time, respectively). The number of defects (linker vacancies) was controllable through regulation of the concentration of the HCl aqueous solution and the irradiation time. The morphology of as-prepared samples was characterized with scanning electron microscopy (SEM). As shown in Figs. 2a and b, UiO-66_{ST} shows a regular octahedron shape with an average diameter of around 240 nm. After the microwave irradiation, no obvious change of particle size was observed except that the particles turned to a truncated octahedron shape with a rough surface, indicative of the etching phenomenon. The crystal structures of UiO-$66_{MW\text{-}0.5M1h}$ and UiO-66_{ST} were determined with powder X-ray diffraction (PXRD). Figs. 2c and d shows that both UiO-$66_{MW\text{-}0.5M1h}$ and UiO-66_{ST} have the same crystal system and cell parameters without any impurity, which match very well with the simulated PXRD pattern of a pure crystalline UiO-66 built-up in a cubic unit-cell with a *Fm3m* space group [11]. It is also mentioned that varying the concentration of the HCl aqueous solution and the irradiation time did not change the crystal structures of samples with slight decrease of the intensity possibly because of the increase of the defects (Fig. S1 in Supporting information).

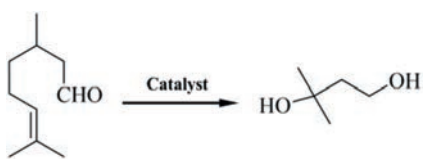

Fig. 1. Conversion of citronellal to 3-methyl-1,3-butanediol.

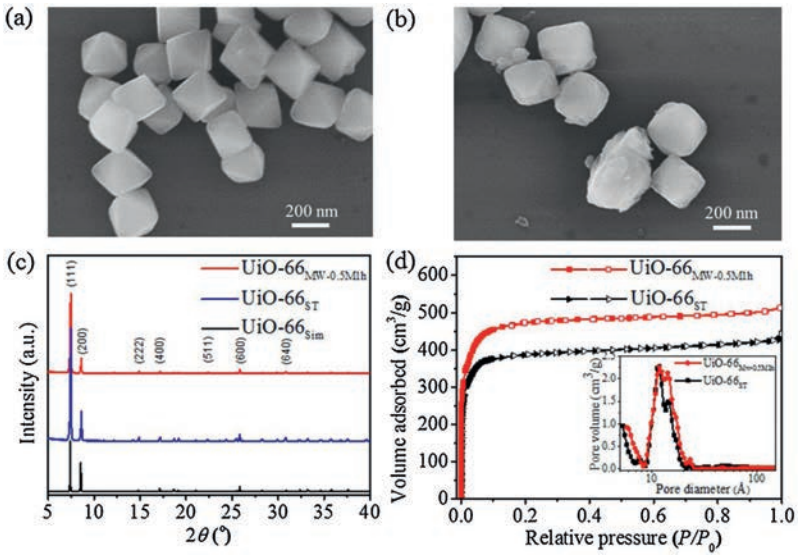

Fig. 2. SEM images of UiO-66 without (a, UiO-66_{ST}) and with (b, UiO-$66_{MW\text{-}0.5M1h}$) the microwave treatment; (c) PXRD patterns of UiO-$66_{MW\text{-}0.5M1h}$ and UiO-66_{ST}, and simulated pattern of UiO-66; and (d) N_2 adsorption/desorption isotherms of the UiO-$66_{MW\text{-}0.5M1h}$ and UiO-66_{ST} (Inset: the corresponding pore diameter distribution curves).

The specific surface area and porosity of UiO-$66_{MW\text{-}0.5M1h}$ and UiO-66_{ST} were measured through N_2 adsorption/desorption isotherms (Fig. 2d). The pore volume and specific surface area of pristine UiO-66_{ST} is 0.58 cm^3/g and 1564 m^2/g, respectively, higher than those calculated from the perfect UiO-66 structure (0.426 cm^3/g and 954 m^2/g). This is reasonable because acetic acid used during the synthesis of UiO-66_{ST}, which served as a modulator to create the ligand defect to increase the pore volume and surface area of MOFs [21]. After treated with the microwave in the HCl aqueous solution (0.5 mol/L for 1 h), the pore volume and specific surface area of MOF were increased significantly to 0.71 cm^3/g and 1864 m^2/g, indicating more ligand defects were created. Pore size distribution also showed that the pore size shifted positively and mesopores centred at 2.3 nm were observed, confirming the presence of more ligand vacancies.

The number of ligand defects could be calculated from thermogravimetric analysis (TGA), which is more efficient to investigate the study defects in MOFs since the weight loss with TGA directly reflect the number of ligands present in defective MOFs. The numbers of defects were calculated according to the method as described by Lillerud and co-authors [15,22]. The formula of fully dehydroxylated UiO-66 with the perfect structure is $Zr_6O_6(BDC)_6$ (BDC represents benzene-dicarboxylate) and each Zr_6 cluster is coordinated with 12 linkers. TGA curves of as-prepared samples were normalized so that end weight (weight percentage of ZrO_2) and weight of perfect UiO-66 were equal to 100 and 220.2 wt%, respectively (Fig. 3a and Fig. S2 in Supporting information). The average defect per cluster for UiO-66_{ST} is 1.8, which means that, on average, 1.8 out of 12 linkers were removed for each Zr_6 clusters in a unit cell. This result shows the modulation method could produce some linker vacancies to certain extent. After treated with the microwave in 0.5 mol/L HCl solution for 1 h, average defect per cluster for UiO-66 increased obviously to 5.0, indicating that averagely 5 out of 12 linkers were removed in the UiO-$66_{MW\text{-}0.5M1h}$. It should be mentioned that the maximum defect of linkers is 6.0 to maintain a 3D framework for UiO-66. The effect of the concentration of HCl solution and the microwave irradiation time on the defects of UiO-66 was investigated as well, shown in Fig. 3b and Fig. S2. These results show that increasing the irradiation time and the concentration of HCl solution can increase the number of linker defects, but UiO-$66_{MW\text{-}0.5M1h}$ displays the largest specific surface area with desirable linker vacancies. Additionally, in the absence of HCl, the number of linker defects is only 2.9, close to that of pristine UiO-66 but less than that in the presence of 0.5 mol/L of HCl. This result also demonstrates that the formation of linker defects is induced by HCl and promoted by the microwave irradiation. Whatever, the microwave-assisted acid induction represents an effective method to create rich linker vacancies.

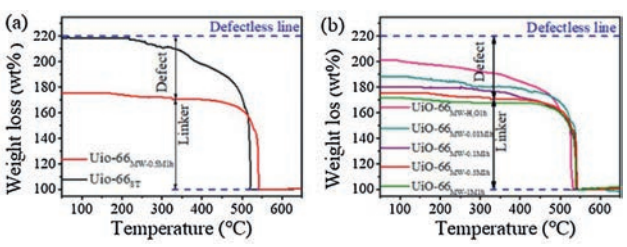

Fig. 3. Normalized TGA results of UiO-66_{ST} (a), and defective UiO-$66_{MW\text{-}mM1h}$ (b) prepared with different acid concentrations.

In general, thermal stability of MOF would be compromised with the presence of defects, which can be reflected from TGA data. Interestingly, in our case, the thermal stability of defective UiO-66 increases, where the decomposition temperature under air shifts from 370 °C (UiO-66_{ST}) to around 450 °C (UiO-$66_{MW\text{-}0.5M1h}$). Feng *et al.* [16] previously reported that defective UiO-66 prepared with the hemilabile linker showed improved thermal stability as well, which was attributed to presence of sulfate groups as evidenced by Density functional theory (DFT) calculations. Herein, we propose three reasons might be responsible for the stabilization of defective UiO-66. First, the instability of previous defective MOFs was resulted from the presence of larger domains of missing linker defects, which would be detrimental to the stability of MOF structures. Beneficial from the homogeneous action on the framework of the microwave, ordered small defects could be created within the structures of UiO-66, so that the stability would not decrease [23]. Second, the microwave irradiation might promote the reconstruction to stabilize the frameworks. This is as evidenced by comparison with TGA curves between pristine UiO-66 and UiO-66 treated in pure water under microwave, which exhibits the thermal stability slightly improved after microwave irradiation (Fig. S3 in Supporting information). Third, chloride may

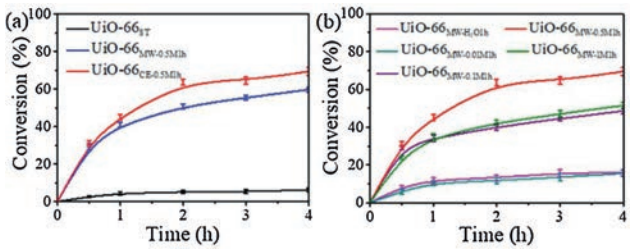

Fig. 4. Citronella conversion rate of UiO-66 as catalyst, under different heat treatment methods (a), different concentrations of hydrochloric acid (b).

play the similar role in the stabilization of the UiO-66 frameworks with the sulfate groups as described by Feng *et al.* [19]. By surveying the TGA results of as-prepared samples, the pristine UiO-66 still contains monocarboxylate modulators (acetate), which will decompose over a range of 200−350 °C. After treated in the HCl solution, very less weight loss was observed in this range, indicating acetate was mostly removed and the frameworks would be compensated with chloride, which might stabilize the structure of defective UiO-66 [22].

Abundant linker vacancies within UiO-66 will expose more unsaturated Zr active sites as Lewis acids, encouraging us to extend their catalytic application. Citronella is a natural product from plants, conversion of which represents a sustainable route for production of feedstocks [17,24]. Hence, we selected the "ene-type" cyclization of citronella to 3-methyl-1,3-butanediol as a model reaction to test the catalytic acidity of defective UiO-66. All samples were activated under vacuum at 200 °C for 12 h before experiment to fully dehydroxylate the inorganic clusters for exposure of unsaturated active sites. As seen from Fig. 4a, the pristine UiO-66 before microwave irradiation only shows extremely low conversion (5.4%) after 4 h; whereas for UiO-$66_{MW\text{-}0.5M1h}$, the conversion can reach 68.1% under the same conditions, fully confirming that the linker vacancies within UiO-66 can significantly improve the activity of Lewis acid. To clarify the function of the microwave, pristine UiO-66 was also treated in HCl solution for 1 h without microwave irradiation (noted as UiO-$66_{CE\text{-}0.5M1h}$). Compared with UiO-$66_{MW\text{-}0.5M1h}$, UiO-$66_{CE\text{-}0.5M1h}$ exhibits a conversion of 54.6% at the same condition, 13.5% less than UiO-$66_{MW\text{-}0.5M1h}$ confirming that the microwave irradiation would result in more active sites. The influence of the concentration of HCl solution and the microwave irradiation time on the catalytic activity of defective UiO-66 was also investigated. Without or with less HCl, the as-formed UiO-66 merely displayed very limited improvement of the catalytic activity with a conversion of around 14.8% after 4 h. Increasing the concentration of HCl would further improve the activity because of the increase of linker defects to expose more Lewis acid active sites. The optimal concentration is 0.5 mol/L because of highest specific surface area. With further increasing the concentration, the structure possibly collapse to some extent to decrease the surface area so as to screen some active sites even more linkers were lost. The trend of the effect of treatment time on the activity is similar with that of the concentration of HCl (Fig. S4 in Supporting information).

The leaching test was further carried out for UiO-$66_{MW\text{-}0.5M1h}$, where no reaction happened after the catalyst was removed (Fig. S5 in Supporting information), confirming the heterogeneous nature of defective UiO-66. The microwave-assisted acid-induction method was further to applied to MOF-808, a larger porous Zr-based MOF formed by coordination between Zr_6 cluster and 1,3,5-benzene-tricarboxylic acid (H_3BTC) with a formula of $Zr_6O_5(OH)_3(BTC)_2(H\text{-}COO)_5$. The MOF-808 nanoparticles also underwent obvious surface roughness after treated in 0.1 mol/L HCl solution with microwave (Fig. S6 in Supporting information). When applied to cyclization of citronella, the conversion for MOF-808 reaches 81.1%, 40% higher than that for pristine MOF-808, illustrating more acidic active sites were exposed after the microwave-assisted acid treatment(Fig. S9 in Supporting information).

In summary, we have demonstrated that a post-treatment method could be applied to creating linker vacancies within stable Zr-based metal organic frameworks including UiO-66 and MOF-808 through microwave-assisted acid induction, and by changing the concentration of hydrochloric acid and the time of microwave in the post-treatment, the amount of defects can be controlled effectively. As well as, the surface morphology of MOF samples after post-treatment changed to a certain extent and the specific surface area was greatly increased. The results of catalytic performance test shows that the MOF with abundant defects have better catalytic performance, and they have good stability.

Declaration of competing interest

The authors declare that they have no known competing financial interests or personal relationships that could have appeared to influence the work reported in this paper.

Acknowledgments

This work was supported by the National Natural Science Foundation of China (No. 21573063), the Hunan Provincial Natural Science Foundation of Youth Fund (No. 2020JJ3002), Open Fund from Hunan Provincial Key Laboratory of Advanced Materials for New Energy Storage and Conversion (No. 2018TP1037_201902), and the Training Program of Hunan University of Youth Fund.

Appendix A. Supplementary data

Supplementary material related to this article can be found, in the online version, at doi:https://doi.org/10.1016/j.cclet.2020.06.042.

References

[1] Q.L. Zhu, Q. Xu, Chem. Soc. Rev. 43 (2014) 5468–5512.
[2] A.J. Howarth, A.W. Peters, N.A. Vermeulen, et al., Chem. Mater. 29 (2016) 26–39.
[3] W. Tan, T. Wei, J. Huo, et al., ACS Appl. Mater. Interfaces 11 (2019) 36782–36788.
[4] Y. Zhou, Z. Li, Y. Liu, J. Huo, S. Wang, ChemSusChem 13 (2020) 1746–1750.
[5] Y.B. Huang, J. Liang, X.S. Wang, R. Cao, Chem. Soc. Rev. 46 (2017) 126–157.
[6] M.H. Sun, S.Z. Huang, L.H. Chen, et al., Chem. Soc. Rev. 45 (2016) 3479–3563.
[7] M.I. Nandasiri, S.R. Jambovane, B.P. McGrail, H.T. Schaef, S.K. Nune, Chem. Rev. 311 (2016) 38–52.
[8] X. Lian, Y. Fang, E. Joseph, et al., Chem. Soc. Rev. 46 (2017) 3386–3401.
[9] P. Jin, W. Tan, J. Huo, et al., J. Mater. Chem. A 6 (2018) 20473–20479.
[10] C. Prestipino, L. Regli, J.G. Vitillo, et al., Chem. Mater. 18 (2006) 1337–1346.
[11] J.H. Cavka, S.R. Jakobsen, U. Olsbye, et al., J. Am. Chem. Soc. 130 (2008) 13850–13851.
[12] D. Feng, W.C. Chung, Z. Wei, et al., J. Am. Chem. Soc. 135 (2014) 17105–17110.
[13] Z. Guo, C. Xiao, R.V. Maligal-Ganesh, et al., ACS Catal. 4 (2014) 1340–1348.
[14] Y. Pak, W. Park, S. Mitra, et al., Small 14 (2018) 1703176.
[15] F. Vermoortele, R. Ameloot, A. Vimont, et al., Chem. Commun. 47 (2011) 1521–1523.
[16] F. Vermoortele, B. Bueken, Gl. Le Bars, et al., J. Am. Chem. Soc. 135 (2013) 11465–11468.
[17] M. Vandichel, J. Hajek, F. Vermoortele, et al., CrystEngComm 17 (2015) 395–406.
[18] S. Dissegna, K. Epp, W.R. Heinz, G. Kieslich, R.A. Fischer, Adv. Mater. 30 (2018) 1704501.
[19] X. Feng, J. Hajek, H.S. Jena, et al., J. Am. Chem. Soc. 142 (2020) 3174–3183.
[20] F. Liang, Y. Shuai, Z. Liang-Liang, et al., J. Am. Chem. Soc. 140 (2018) 2363–2372.
[21] H. Wu, Y.S. Chua, V. Krungleviciute, et al., J. Am. Chem. Soc. 135 (2013) 10525–10532.
[22] G.C. Shearer, S. Chavan, S. Bordiga, et al., Chem. Mater. 28 (2016) 3749–3761.
[23] C.G. Piscopo, A. Polyzoidis, M. Schwarzer, S. Loebbecke, Microporous Mesoporous Mater. 208 (2015) 30–35.
[24] L. Alaerts, E. Séguin, H. Poelman, et al., Chem. Eur. 12 (2016) 7353–7363.